

Published in final edited form as:

Medchemcomm. 2012 June 1; 3(6): 685–690. doi:10.1039/C2MD00297C.

A NIR Dye for Development of Peripheral Nerve Targeted Probes

Tiffany P. Gustafson^a, Ying Yan^b, Piyaraj Newton^b, Daniel A. Hunter^b, Samuel Achilefu^a, Walter J. Akers^a, Susan E. Mackinnon^b, Philip J. Johnson^{b,*}, and Mikhail Y. Berezin^{a,*}

^aDepartment of Radiology, Washington University in St. Louis School of Medicine, St. Louis, MO 63110, USA

^bDepartment of Surgery, Division of Plastic and Reconstructive Surgery, Washington University in St. Louis School of Medicine, St. Louis, MO 63110, USA

Abstract

Current imaging modalities lack the ability to quickly assess and classify nerve injury for predicting favourable versus unfavourable healing outcomes, which could minimize episodes of chronic pain and loss of function by allowing for early intervention. Thus, the development of a technique to noninvasively assess peripheral nerve damage is of critical importance. While the development of nerve specific near infrared (NIR) molecular probes capable of such diagnostics constitutes our long term goal, initial studies to identify a NIR dye for constructing such a probe are required. We have evaluated the properties of a novel highly hydrophilic and functionalizable polymethine dye, and its more hydrophobic analogue indocyanine green, within the sciatic nerve of rats following intra-nerve injection. The reporting ability of both dyes at critical depths for nerve imaging, the importance of hydrophilicity on dye transport through nervous tissue, and their toxicity – or lack thereof – to the neural environment have been evaluated. The results suggest that the novel NIR dye is an appropriate fluorescent reporter for use in designing nerve-specific optical molecular probes for non-invasive diagnosis and classification of nerve injury.

Introduction

Peripheral nerve injuries often result from minor accidents, traumatic injuries, surgery and diseases affecting an estimated 600,000 patients each year.^{1, 2} Successful treatment relies on the ability to quickly assess and classify nerve injury as having a favourable (injuries capable of healing over time, Sunderland grade 1–3) or unfavourable outcome (injuries needing immediate intervention, Sunderland grade 4–5).³ The current methods for non-invasive diagnosis of peripheral nerve injuries, including computed tomography (CT),^{4, 5} ultrasound (US),^{6–10} and magnetic resonance imaging (MRI)^{11–15} can allow for their visualization and evaluation. However, dependence upon gross changes to tissue morphology (swelling, edema, etc.) limits the utility of these imaging modalities to identifying the location of acute nerve injuries, but does not allow for classification of injuries, which is based upon loss of morphological features – i.e. axons, myelin, endoneurium, etc.^{3, 16} This leads to a wait-and-see approach which delays treatment and commonly results in suboptimal outcomes in functional recovery following surgical repair.^{2, 17} Thus, the development of a technique to noninvasively assess nerve damage, which can provide correlation to the extent of axonal injury and allows for its overall

This journal is © The Royal Society of Chemistry [year]

Fax: 1-314-747-5191; Tel: 1-314-747-0701; berezinm@mir.wustl.edu. Fax: 1-314-747-0579; Tel: 1-314-362-1275; johnsonp@wudosis.wustl.edu.

[†]Electronic Supplementary Information (ESI) available: Experimental description of the synthesis of LS601, small animal surgical and imaging, procedures, and histomorphometry. See DOI: 10.1039/b000000x/

classification, is one of the most pressing needs in the treatment of peripheral nerve injuries.^{18–20}

Unlike current clinical imaging modalities, optical imaging is capable of assessing tissue pathology *in vivo* with high sensitivity at the molecular level, permitting visualization of nerve morphology.^{21–23} This has been demonstrated through the use of Thy1-XFP transgenic rodents producing a fluorescent protein (XFP) expressed in their axons.^{24, 25} This model suffers from three major drawbacks: i) emission is in the visible spectrum, suffering from high levels of autofluorescence; ii) high scattering limits detection through skin and in deep tissue; and iii) the presence of exogenous genes in the model limits the potential for clinical translation.

More recently the design and development of contrast agents for image guided surgery has provoked interest, especially in an effort to minimize accidental nerve damage during surgery.^{1, 26–28} These efforts have led to the design of the first visible^{29, 30} and far red^{1, 26} (500–650 nm) emitting optical contrast agents and targeted probe for peripheral nerve identification. While these approaches allow for visualization of an exposed nerve they do not provide injury classification and have limited use in non-invasive imaging procedures, as their emission remains within the visible region.

The utilization of imaging agents in the near-infrared (NIR) range (700–950 nm) extends imaging capabilities from a few millimetres (visible range) up to several centimetres in depth due to attenuated scattering and a reduced number of endogenous fluorophores within this range.^{21, 31–36} This provides a unique opportunity to carry out *in vivo* imaging using non- to minimally invasive procedures to rapidly distinguish between normal and diseased/damaged tissue.^{21–23, 37} As a result, optical imaging, using NIR dyes as fluorescent reporters, has become increasingly utilized in preclinical and clinical studies.

Based on light-tissue interaction³⁸ an ideal optical probe for the diagnosis of peripheral nerve injuries should include a NIR fluorophore (dye) which can be attached to a nerve specific targeting moiety, such as an antibody or small peptide, to enhance selective accumulation and/or assist in moving the probe through the blood nerve barrier (BNB). The fluorophore should have limited or no effect on movement of a targeted probe within neural tissue. Additionally, it should allow for non- to minimally invasive detection of NIR emission at clinically relevant depths and be non-neurotoxic. To our knowledge no such probe has been identified. The design of this probe is the long term goal of this project.

The first step towards the initial development of a nerve targeted optical probe has been to investigate two polymethine based fluorophores. The FDA approved indocyanine green (ICG), which is extensively utilized for *in vivo* imaging,^{39–41} and its hydrophilic analogue prepared in our laboratory, LS601⁴² (Figure 1, synthesis is given in Supporting Information, Scheme S1) previously described in patent literature as a dye for NIR absorbing ink⁴³ were used. Polymethine dyes are relatively easy to synthesize and their skeleton offers an excellent scaffold for introducing functionalities for incorporation into optical probes. In the course of this work, we evaluated the potential of these dyes as NIR reporters in the development of nerve targeted optical imaging probes and have determined how these dyes interact with the neural environment.

Results & Discussion

Targeted probes for optical imaging of peripheral nerves will carry a NIR fluorescent dye, which can impact the biological properties of the probe. As such, the dyes must be carefully evaluated to identify those which facilitate development of targeted probes maintaining the

above outlined ideal properties for peripheral nerve injury assessment. Herein, we provide an evaluation of NIR polymethine dyes with similar optical properties (Table 1) but principally different *in vivo* behaviour. ICG and LS601 differ by hydrophilicity, because of additional hydrophilic groups (carboxylates) on LS601, and the ability of LS601 to be conjugated to a targeting moiety via at least one of these groups as we demonstrated previously.⁴²

The difference in hydrophilicity between LS601 and ICG is clearly demonstrated through comparison of the retention times using reverse phase HPLC (3.11 and 5.32 min respectively, Supporting information Fig. S1 and Fig. S2).

Imaging of the Sciatic Nerve *in vivo*

To demonstrate detection of NIR emission at depths clinically applicable to peripheral nerve injury we evaluated the dyes in the rat sciatic nerve, at approximately 1 cm below the rat's skin surface. The depth of most commonly injured and clinically relevant peripheral nerves of the extremities is up to 2 cm,² placing us within the appropriate range. The dyes were injected into the sciatic nerve of transgenic Sprague Dawley rats expressing GFP under the regulation of the Thy1 promoter found in neurons. Intra-neural injection guaranteed each dye was present within the nerve, allowing for direct visualization of fluorescence in nerve tissue.²⁵ Rats were broken into 6 groups, as defined in the supplemental information, and received an injection of either LS601 or ICG. Beyond the fluorophore injected the groups differed only by the time of sacrifice. Initial NIR optical imaging of each limb was performed within 2 h of dye injection. This time gap was due to the logistics of moving all animals from surgery and the fluorescence dissecting microscope to the planar imaging system. Fluorescence imaging showed a strong signal from the injected dyes, demonstrating that both dyes remained at or near the site of injection (Figure 2, panel D shows a representative 2 h post injection (PI) image). As expected, GFP was not detectable at these depths. NIR fluorescence was not detected in the control group because of the relative absence of endogenous emitters in the NIR range.

At longer time points, 20 – 48 h PI (Figure 2, panels A–C) the differences between the two dyes became apparent. While ICG remained largely in the same location, as indicated by a single high intensity spot at the site of injection (ROI #4, Figure 2, panel D left), the more hydrophilic LS601 appears to migrate along the sciatic nerve. Two clearly observed high intensity fluorescent spots at ROI #2 and #5 along the sciatic nerve verifies the proximal and distal movement of LS601 (Figure 2, panel D right). In all nerves there was an overall decrease in fluorescence signal over time. A larger decrease in fluorescence intensity of LS601 further indicates its migration along the nerve into deeper tissue, as the nerve proximally merges into the spinal cord and distally becomes buried in muscle. By 48 h PI fluorescence from LS601 can no longer be seen, yet hydrophobic ICG remains intensely fluorescent at the site of injection (data not shown). Results were consistent over 3 sciatic nerves.

These data illustrate the potential of NIR imaging with fluorescent reporters at depths relevant to peripheral nerves via non-invasive transdermal imaging, even with a relatively simple planar imaging system. Spatial and depth resolution of NIR imaging could be further improved by utilizing more complex methods such as diffuse optical tomography.^{45, 46}

Effect of Dye Hydrophilicity

The use of hydrophilic dyes to eliminate nonspecific binding in optical imaging is well accepted. We recently demonstrated that the hydrophilicity of polymethine based NIR fluorophores directly influences the pharmacokinetics and distribution of their fluorophore-

biomolecule conjugates (a targeted optical probe), specifically its ability to move out of the vasculature.³³ More hydrophobic dyes including ICG with a binding constant to albumin $K \sim 556,000 \text{ M}^{-1}$, were retained in the vasculature through binding to albumin, while the hydrophilic analogues with $K < 15,000 \text{ M}^{-1}$ quickly extravasated into the surrounding tissue. This study clearly demonstrated that a probe's ability to reach its target can be effected by the attached fluorescent reporter.

Unlike the vasculature, the neural environment is unique and has not been previously explored in these regards. Endoneurial fluid contains many proteins which are not present in other systems; determining whether the same effect of hydrophilicity applies is critical in the design of nerve specific probes. While the hydrophilicity of the dye may affect its ability to cross the blood-nerve-barrier (BNB) we rationalized that hydrophilicity may also influence the ability of a small targeted probe to move within nervous tissue, and thus to reach a specific target. Therefore, the hydrophilic dye LS601, with low binding affinity to albumin ($K \sim 10,000 \text{ M}^{-1}$ see Supporting Information Fig. S3) and easiness to conjugation was selected for this study.

We evaluated the effects of hydrophilicity on dye movement within the nerve to determine its suitability for incorporation into an NIR nerve targeted optical probe as a reporter. First, we utilized dissection images of each sciatic nerve. *In vivo* images were taken directly following injection and at either 6 h or 24 h PI (Figure 3). To fully visualize dye distribution along the sciatic nerve its entire length was exposed from the sciatic notch to the most distally exposed portions of the tibial, sural and peroneal nerves (just proximal to where these nerves enter the muscle) at the time of animal sacrifice (6 or 24 h PI). For all nerves, both LS601 and ICG remain at, and proximal to, the injection site PI. This is expected as the injection was made in a proximal direction. After 24 h ICG remained at its original location. In contrast, noticeable migration of LS601 in both the antero- and retrograde directions ($\sim 1 \text{ mm}$) was observed at 6 h PI. After 24 h LS601 appears to have moved 3–4 mm in both directions from the injection site, indicating that movement may be at a steady rate of $\sim 0.1\text{--}0.15 \text{ mm/h}$, both distal and proximal as shown in Figure 3 (results were consistent over 3 sciatic nerves).

Second, following *in vivo* imaging each sciatic nerve was harvested to verify the impact of dye hydrophilicity on its ability to migrate along the nerve using confocal microscopy. Multiple images of each nerve were taken at the proximal and distal ends as well as the middle of the nerve near the site of injection (Figure 4). Fluorescence from ICG appears to remain near the injection site, correlating with results from *in vivo* imaging (Figure 3). Highest intensity emission was detected at the middle of the nerve, with significantly lower emission at the proximal and no emission at the distal site. This result is expected for a compound which adheres to surrounding tissue, as injections were made proximally, and unless the dye distributes across the nerve the maximum intensity remains at the injection site. The fact that no fluorescence is seen distal to the site of injection confirms that the dye did not migrate. Additionally, ICG does not appear to diffuse transversely across the diameter of the nerve. It is likely that ICG, because of its hydrophobic nature, “sticks” to myelin or other nerve tissue components. It has previously been shown that hydrophobic fluorophores have a high affinity to the myelin sheath in the peripheral and central nervous systems.^{1, 29, 30} In fact, this has been the basis for the first contrast agent designed for image guided surgery to prevent accidental nerve damage.¹ We believe that such hydrophobic contrast agents are suitable for highlighting nerves during surgery, but they have limited use for incorporation into targeted probes, where high mobility of the probe within the neural environment will be required to reach the tissue of interest.

Hydrophilic LS601, unlike ICG, appears to freely diffuse throughout the nerve, migrating in both antero- and retrograde directions (Figure 3, panel D). This is demonstrated both *in vivo* and by confocal imaging of LS601 injected nerves harvested 6 h PI. The most intense NIR fluorescence detected from LS601 at 6 h PI was within the proximal end of the nerve, with lower intensity at the distal end, and no detectable fluorescence near the site of injection (middle) (Figure 4). Additionally, the fluorescence signal diffused transversely across the nerve, further confirming low binding affinity of the dye to nerve tissue. Migration of the dye resulted in too low of a concentration remaining at 24 h PI to allow for confocal imaging. The hydrophilic nature of LS601 suggests its retention with the endoneurial fluid rather than becoming trapped within connective tissue of the nerve. The endoneurium of rats is composed of 70% water which is distributed between intracellular and extracellular components, with extracellular water being both free and part of a hydrated gel-like ground substance.^{47, 48} The free movement of LS601 throughout the nerve indicates that a hydrophilic dye would be an appropriate candidate for incorporation into an optical probe specific to nervous tissue/structures. In contrast, hydrophobic dyes would interfere with the specificity of targeting probes in neural applications, because of their propensity to “stick” to non-specific hydrophobic structures. While the small numbers of animals used in this study precludes statistical evaluation, the results clearly and reproducibly demonstrate the difference between hydrophilic and hydrophobic molecular transport in nerves.

Neurotoxicity of LS601

To incorporate LS601 into a targeted imaging agent it must be non-neurotoxic, it cannot cause axonal degeneration or injury to the morphology of the nerve. Both LS601 and saline (as a control) were directly injected into the sciatic nerves of Thy1-GFP rats. Two weeks post injection the nerves were harvested and evaluated, along with an untreated nerve, by histomorphometry. The results demonstrate that nerves treated with LS601 retain normal fiber architecture with a complete absence of Wallerian degeneration and demyelination (Figure 5), showing no evidence of any axonal injury. The lack of histological damage and observation of normal morphology suggests no loss of nerve function was induced as a result of the injected dye. Further, comparison of the quantified histomorphometric parameters for the nerve injected with LS601 vs. the controls (saline injection and an untreated nerve), demonstrated no differences (Table 2). Nerves treated with LS601 have almost identical parameters to those receiving saline and normal non-treated nerves, indicating that the dye lacks neuronal toxicity. The small variability in the morphometric parameters is expected, as a result of natural biological variability between animals. Therefore, the morphological data indicate no evidence of injury.

Conclusions and Future Directions

LS601 was designed in our laboratory to have similar photophysical properties to ICG while allowing for facile coupling to a targeting molecule, such as a polypeptide or antibody, under aqueous conditions. Attachment of LS601 to targeting moieties (peptides, antibodies, and proteins) has already been carried out using standard NHS based protocols.⁴² The above results show that, following attachment to a targeting moiety, the dye LS601 should not interfere with the movement of the probe within the nerve and will allow for detectable contrast at the tissue of interest.

On the whole, LS601 appears to exhibit the appropriate qualities of a NIR dye for incorporation into an optical probe, for the diagnosis of peripheral nerve injuries. Having identified the dye, our next task is to select several potential markers for neuronal structures/tissues which can be indicative of injury. Nerve injury small animal models such as a crush and transection injuries to the sciatic and facila nerves will be explored. Successfully

targeting these tissues and an optimized method of probe administration will allow for classification of injury as having favourable or unfavourable outcomes, leading to more timely treatment of peripheral nerve injuries. Finally, the utility of the advanced imaging methods, such as diffuse optical tomography, photoacoustics, two-photon optical imaging in combination with targeted probes in nerve imaging will be explored in future studies to increase depth penetration for imaging deep lying nerves.

In summary, we have demonstrated the feasibility of NIR imaging to detect fluorescence, emanating from within the peripheral nerve, at depths critical to their clinical evaluation in humans. By comparing our novel hydrophilic NIR dye LS601 to its FDA approved hydrophobic counterpart ICG, a direct correlation between dye hydrophilicity and its ability to migrate through nervous tissue was demonstrated. Hydrophobic ICG becomes trapped in neuronal tissue and shows no movement from the point of administration. In contrast, LS601 migrated along the nerve in both the antero- and retrograde directions. This movement was confirmed through both *in vivo* and *ex vivo* imaging of the sciatic nerves of Thy1-GFP rats. Histomorphometry demonstrated that nerves treated with LS601 retain normal fiber architecture with an absence of Wallerian degeneration and demyelination, suggesting the dye is not neurotoxic. Overall, we have demonstrated the feasibility of non-invasive imaging at depths clinically relevant to peripheral nerves, and shown that the hydrophilic dye LS601 would be an excellent candidate for use in the design of NIR targeted optical probes for the non-invasive visualization of nerves and diagnosis of peripheral nerve injuries.

Supplementary Material

Refer to Web version on PubMed Central for supplementary material.

Acknowledgments

We gratefully acknowledge financial support from: the National Institutes of Health, National Cancer Institute R21CA149814, National Institute of Neurological Disorders and Stroke R01NS033406, and the Washington University Molecular Imaging Center and National Heart Lung and Blood Institute, a Program of Excellence in Nanotechnology P50CA094056 (HHSN268201000046C).

Notes and references

1. Gibbs-Strauss SL, Nasr KA, Fish KM, Khullar O, Ashitate Y, Siclovan TM, Johnson BF, Barnhardt NE, Tan Hehir CA, Frangioni JV. *Mol Imaging*. 2011; 10:91–101. [PubMed: 21439254]
2. Mackinnon, SE.; Dellon, AL. *Surgery of the Peripheral Nerve*. New York: Thieme Medical Publishers; 1988.
3. Sunderland S. *Brain*. 1951; 74:491–516. [PubMed: 14895767]
4. Baron B, Goldberg AL, Rothfus WE, Sherman RL. *J Comput Assist Tomogr*. 1989; 13:364–365. [PubMed: 2538495]
5. Yu YL, du Boulay GH, Stevens JM, Kendall BE. *Neuroradiology*. 1986; 28:221–236. [PubMed: 3014373]
6. Ernberg LA, Adler RS, Lane J. *Skeletal Radiol*. 2003; 32:306–309. [PubMed: 12719933]
7. Gray AT, Collins AB, Schafhalter-Zoppoth I. *Anesth Analg*. 2003; 97:1300–1302. [PubMed: 14570642]
8. Gray AT, Schafhalter-Zoppoth I. *Reg Anesth Pain Med*. 2003; 28:335–339. [PubMed: 12945028]
9. Sidhu MK, Perkins JA, Shaw DW, Bittles MA, Andrews RT. *J Vasc Interv Radiol*. 2005; 16:879–884. [PubMed: 15947054]
10. Spence BC, Sites BD, Beach ML. *Reg Anesth Pain Med*. 2005; 30:198–201. [PubMed: 15765462]
11. Howe FA, Filler AG, Bell BA, Griffiths JR. *Magn Reson Med*. 1992; 28:328–338. [PubMed: 1461131]

12. Cudlip SA, Howe FA, Griffiths JR, Bell BA. *J Neurosurg.* 2002; 96:755–759. [PubMed: 11990818]
13. Gupta R, Villablanca PJ, Jones NF. *J Hand Surg Am.* 2001; 26:1093–1099. [PubMed: 11721257]
14. Dailey AT, Tsuruda JS, Filler AG, Maravilla KR, Goodkin R, Kliot M. *Lancet.* 1997; 350:1221–1222. [PubMed: 9652565]
15. Maravilla KR, Bowen BC. *AJNR Am J Neuroradiol.* 1998; 19:1011–1023. [PubMed: 9672005]
16. Bain JR, Mackinnon SE, Hunter DA. *Plast Reconstr Surg.* 1989; 83:129–138. [PubMed: 2909054]
17. Mirastschijski U, Vogt PM. *Med Hypotheses.* 2011; 76:110–112. [PubMed: 20851534]
18. Hems TE, Birch R, Carlstedt T. *J Hand Surg Br.* 1999; 24:550–555. [PubMed: 10597930]
19. Rankine JJ. *Clin Radiol.* 2004; 59:767–774. [PubMed: 15351241]
20. Walker FO. *Suppl Clin Neurophysiol.* 2004; 57:243–254. [PubMed: 16106623]
21. Achilefu S. *Technol Cancer Res Treat.* 2004; 3:393–409. [PubMed: 15270591]
22. Frangioni JV. *Curr Opin Chem Biol.* 2003; 7:626–634. [PubMed: 14580568]
23. Klohs J, Wunder A, Licha K. *Basic Res Cardiol.* 2008; 103:144–151. [PubMed: 18324370]
24. Pan YA, Misgeld T, Lichtman JW, Sanes JR. *J Neurosci.* 2003; 23:11479–11488. [PubMed: 14673013]
25. Magill CK, Moore AM, Borschel GH, Mackinnon SE. *Arch Facial Plast Surg.* 2011; 12:315–320. [PubMed: 20855773]
26. Whitney MA, Crisp JL, Nguyen LT, Friedman B, Gross LA, Steinbach P, Tsien RY, Nguyen QT. *Nat Biotechnol.* 2011; 29:352–356. [PubMed: 21297616]
27. Wu AP, Whitney MA, Crisp JL, Friedman B, Tsien RY, Nguyen QT. *The Laryngoscope.* 2011; 121:805–810. [PubMed: 21328585]
28. Pfister BJ, Gordon T, Loverde JR, Kochar AS, Mackinnon SE, Cullen DK. *Crit Rev Biomed Eng.* 2011; 39:81–124. [PubMed: 21488817]
29. Wang C, Wu C, Popescu DC, Zhu J, Macklin WB, Miller RH, Wang Y. *J Neurosci.* 2011; 31:2382–2390. [PubMed: 21325505]
30. Wang C, Wu C, Zhu J, Miller RH, Wang Y. *Journal of medicinal chemistry.* 2011; 54:2331–2340. [PubMed: 21391687]
31. Akers WJ, Zhang Z, Berezin M, Ye Y, Agee A, Guo K, Fuhrhop RW, Wickline SA, Lanza GM, Achilefu S. *Nanomedicine (Lond).* 2010; 5:715–726. [PubMed: 20662643]
32. Berezin MY, Achilefu S. *Chem Rev.* 2010; 110:2641–2684. [PubMed: 20356094]
33. Berezin MY, Guo K, Akers W, Livingston J, Solomon M, Lee H, Liang K, Agee A, Achilefu S. *Biochemistry.* 2011; 50:2691–2700. [PubMed: 21329363]
34. Kou X, Zhang S, Tsung CK, Yang Z, Yeung MH, Stucky GD, Sun L, Wang J, Yan C. *Chemistry.* 2007; 13:2929–2936. [PubMed: 17183599]
35. Zhang Z, Fan J, Cheney PP, Berezin MY, Edwards WB, Akers WJ, Shen D, Liang K, Culver JP, Achilefu S. *Mol Pharm.* 2009
36. Lee J, Bogoy M. *ACS chemical biology.* 2010; 5:233–243. [PubMed: 20017516]
37. Dhaliwal K, Escher G, Unciti-Broceta A, McDonald N, Simpson AJ, Haslett C, Bradley M. *Med Chem Comm.* 2011; 2:1050–1053.
38. Vo-Dinh, T. *Biomedical Photonics Handbook.* Boca Raton, Fla: CRC Press; 2003.
39. Berezin MY, Guo K, Akers WJ, Livingston J, Solomon M, Lee H, Liang K, Agee A, Achilefu S. *Biochemistry.* 2011
40. Weissleder R, Tung CH, Mahmood U, Bogdanov A Jr. *Nat Biotechnol.* 1999; 17:375–378. [PubMed: 10207887]
41. Bremer C, Tung CH, Weissleder R. *Nat Med.* 2001; 7:743–748. [PubMed: 11385514]
42. Gustafson TP, Cao Q, Berezin MY. *Chem Phys Chem.* 2012
43. Japan Pat. JP 63195655 A 19880812. 1988.
44. Benson RC, Kues HA. *Phys. Med. Biol.* 1978; 23:159–163. [PubMed: 635011]
45. Yuan B, Burgess SA, Iranmahboob A, Bouchard MB, Lehrer N, Bordier C, Hillman EM. *Rev. Sci. Instrum.* 2009; 80:043706. [PubMed: 19405665]

46. Gregg NM, White BR, Zeff BW, Berger AJ, Culver JP. *Front. Neuroenergetics*. 2010; 2:1–8. [PubMed: 20162100]
47. Weerasuriya A, Mizisin AP. *Methods Mol Biol*. 2011; 686:149–173. [PubMed: 21082370]
48. Mizisin AP, Weerasuriya A. *Acta Neuropathol*. 2011; 121:291–312. [PubMed: 21136068]

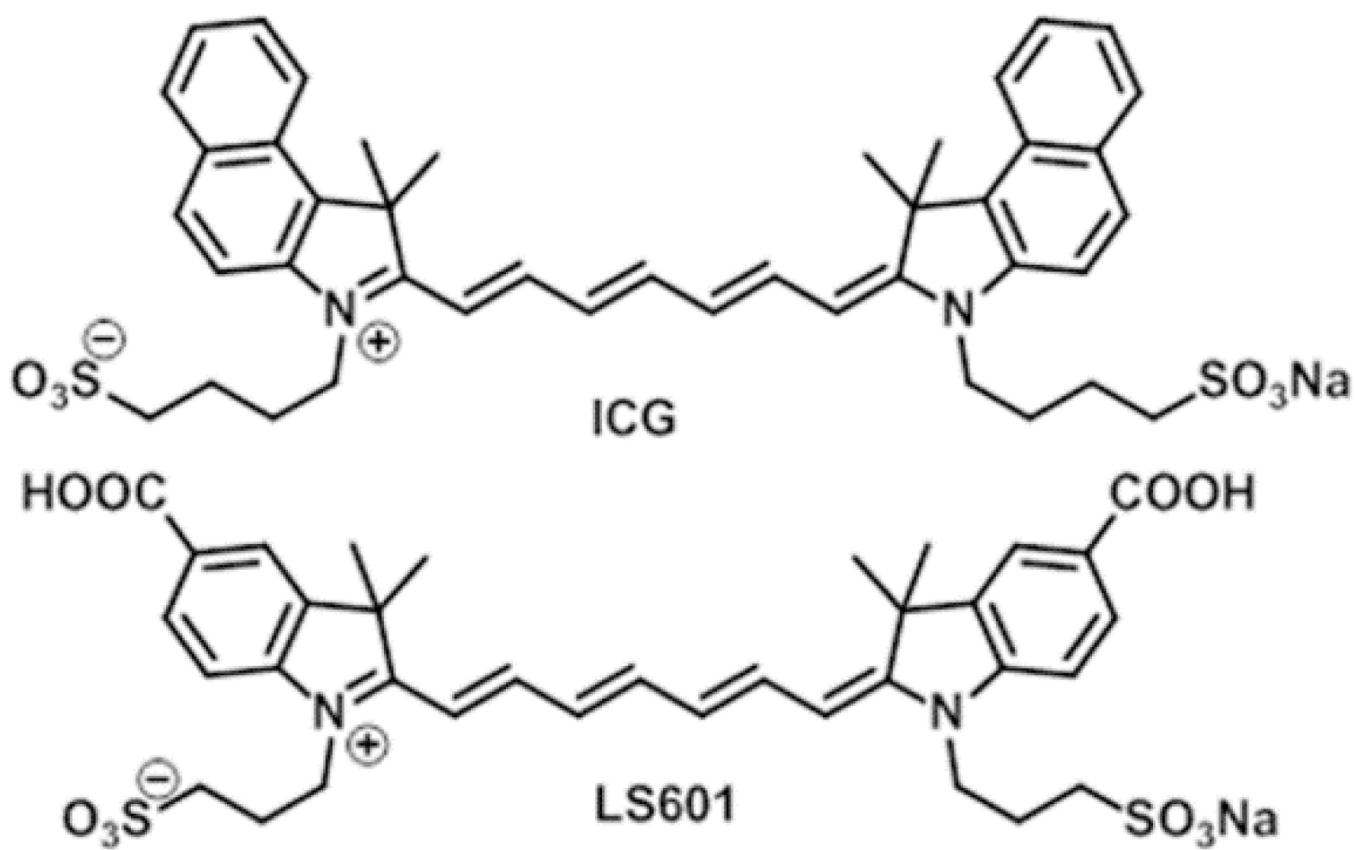


Fig. 1.
Structures of the NIR dyes ICG and LS601

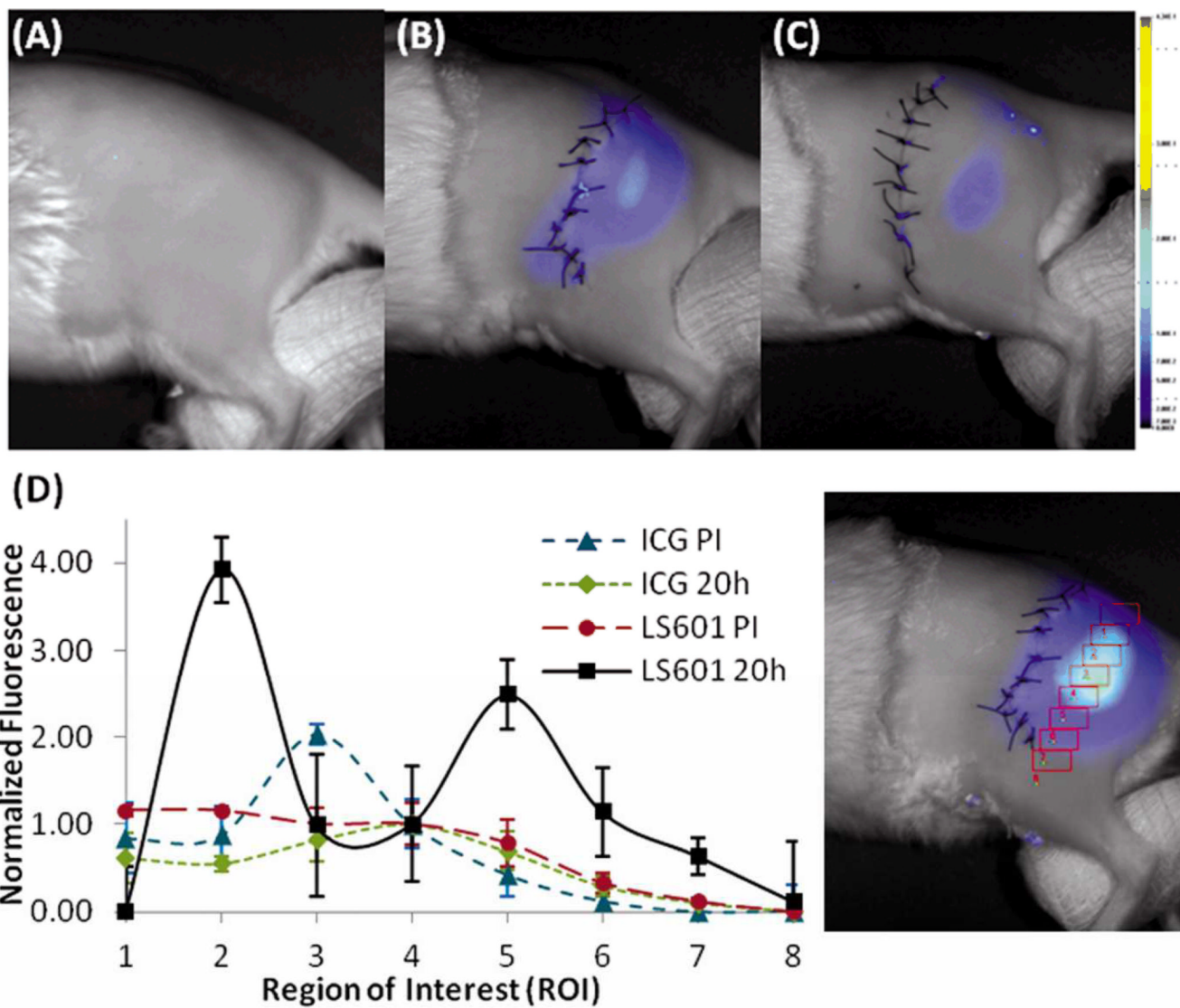


Fig. 2. Fluorescence analysis of transdermal images post injection (PI). Control (A), ICG 20 h PI (B), LS601 20h PI (C). 8 ROI intensity analysis along the sciatic nerve (#1 proximal to #8 distal) indicating movement of LS601 from 1.5 h PI to 20 h PI normalized to ROI #4(D). The same analysis shows that ICG remains at the site of injection.

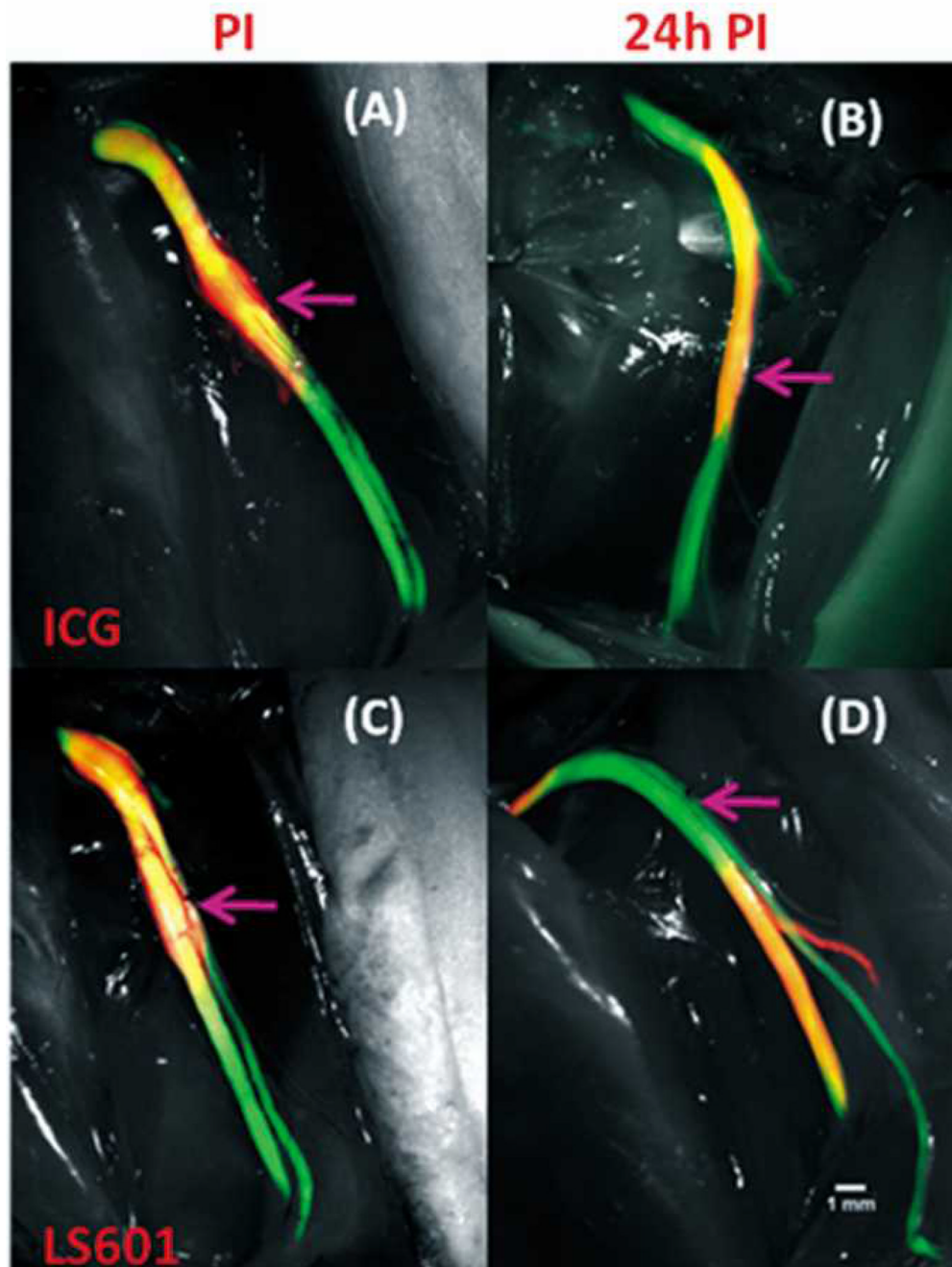


Fig. 3. NIR dye movement along the sciatic nerve of Thy1-GFP rats. Green color indicates GFP emission, red corresponds to NIR emission from LS601. Orange indicates overlap of GFP emission with that of NIR emission from LS601. NIR and GFP fluorescence signal directly correlate, validating placement of dye within the sciatic nerve. 10× Images: ICG post injection (PI) (A), ICG 24h PI (B), LS601 PI (C), LS601 24h PI (D). The arrows indicate injection location.

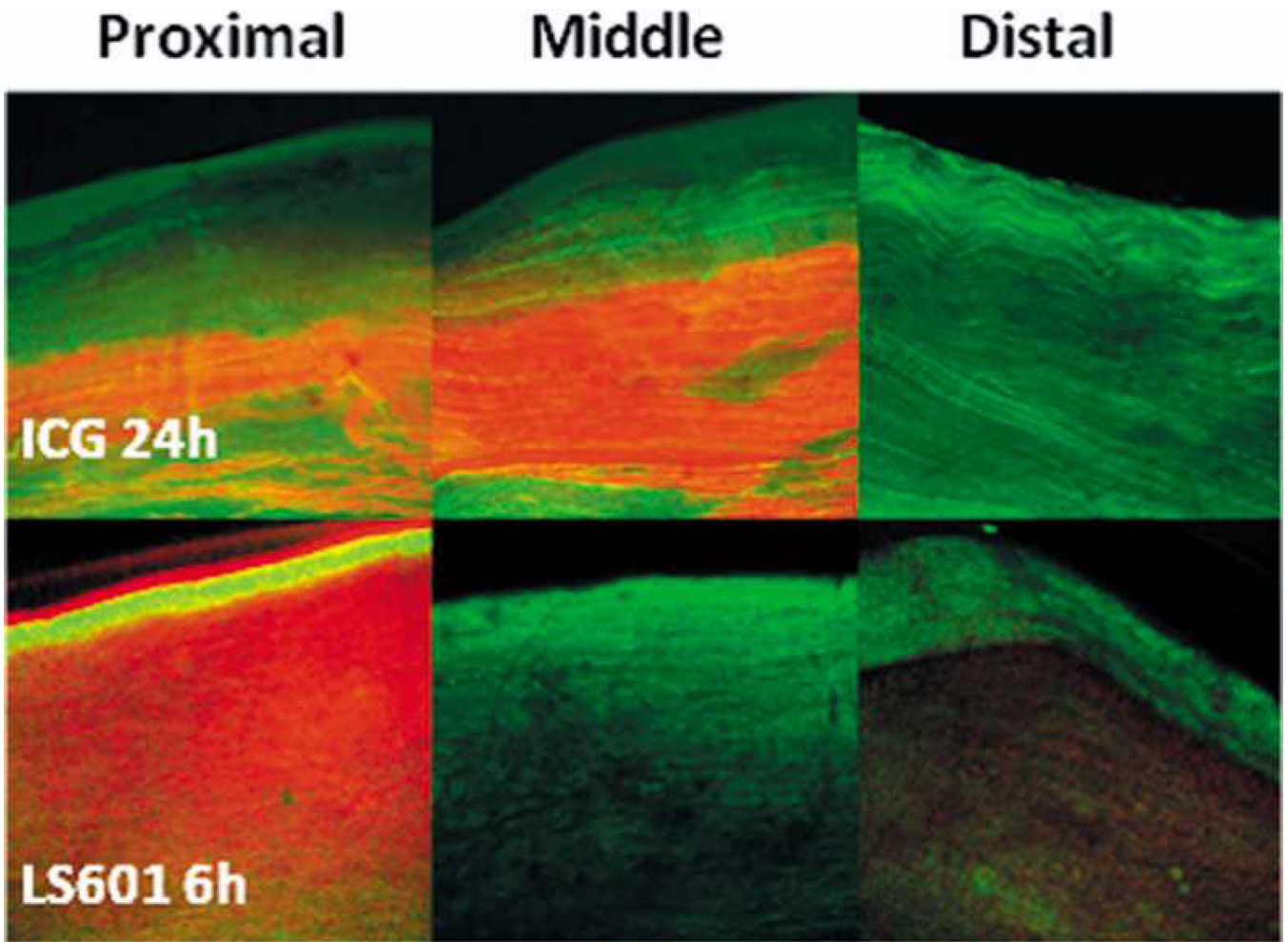


Fig. 4. Representative 10× confocal microscopy images of the proximal, middle, and distal sections of sciatic nerves injected with ICG (top three panels, 24 h PI) or LS601 (bottom three panels, 6h PI). Green color indicates GFP emission, red color corresponds to NIR emission from LS601. Orange to brown color indicates overlap of GFP emission with that of NIR emission from LS601.

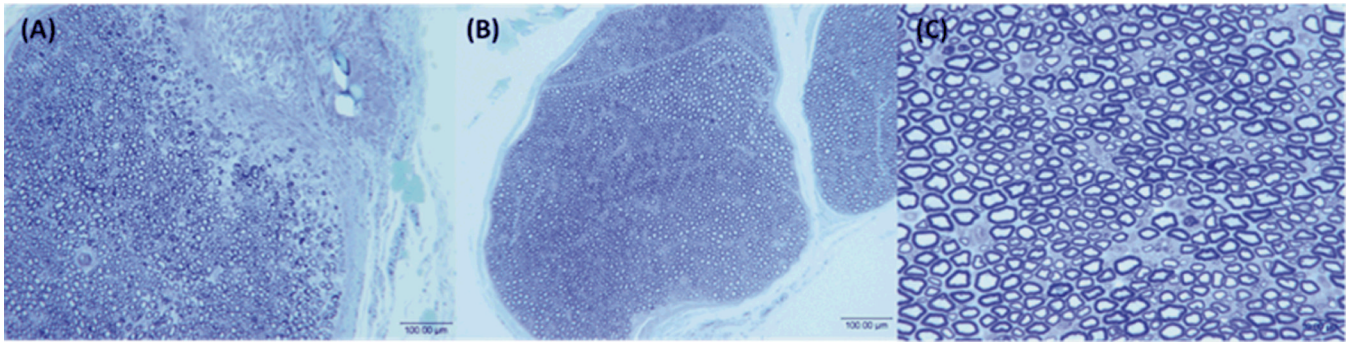


Fig. 5. Representative histological sections from the injection site, injury is due to injection (A) and distal to the injection site at 100× (B) and 400× (C) demonstrate that the dye LS601 is not toxic to healthy nerves.

Table 1

Photophysical properties of NIR dyes in DMSO

Dye	λ_{abs} (nm), ^a	λ_{em} (nm), ^b	ϵ (M ⁻¹ cm ⁻¹), ^c	Φ , ^d
LS601	769	800	161,000	0.20
ICG	794	817	286,000	0.12 ^e

^a λ_{abs} – absorption maxima,^b λ_{em} – emission maxima,^c ϵ - molar absorptivity at the λ_{abs} ,^d Φ -fluorescence quantum yield,^e ϵ_{ref}^{44}